



Functional properties of chitosan-based films

I. Leceta, P. Guerrero, K. de la Caba*

University of the Basque Country (UPV/EHU), Chemical and Environmental Engineering Department, Polytechnic School, Donostia-San Sebastián, Spain

ARTICLE INFO

Article history:

Received 16 September 2011
Received in revised form 28 March 2012
Accepted 11 April 2012
Available online 20 April 2012

Keywords:

Chitosan
Plasticizer
Films
Physico-chemical characterization
Mechanical properties

ABSTRACT

Chitosan-based films plasticized with glycerol were prepared by casting with the aim to obtain environmentally friendly materials for packaging applications. Different contents of glycerol were incorporated into chitosan solutions to improve mechanical properties and all films obtained were flexible and transparent. It was observed that the transparency and good behaviour of the films against UV radiation were not affected by chitosan molecular weight or glycerol content. Moreover, chitosan-based films exhibited excellent barrier properties against water vapour and oxygen, even with the addition of glycerol. The effect of the plasticizer on the properties has been explained using Fourier transform infrared (FTIR) spectroscopic analysis. The changes observed in the intensity of the bands showed that glycerol interacts with chitosan, which could be confirmed by total soluble matter (TSM).

© 2012 Elsevier Ltd. All rights reserved.

1. Introduction

Nowadays there is an increasing interest in biodegradable/compostable polymers from renewable sources due to the environmental problems caused by conventional food packaging materials. Films prepared with these polymers are usually based on polysaccharides, proteins and lipids, which are generally biodegradable, nontoxic, and some of them are effective barriers to oxygen and carbon dioxide, so they can be used as protective coating to maintain food quality and, at the same time, reduce the environmental impact of packaging wastes. Moreover, there is a growing interest to develop materials with antimicrobial character to prevent alterations in food caused by microorganisms' contamination and, in this context, chitosan is an interesting film forming material (Dutta, Tripathi, Mehrotra, & Dutta, 2009).

Chitosan is the second most abundant polysaccharide found in nature and has non-toxic, biodegradable, and antimicrobial characteristics, which are of great interest for packaging purposes. Chitosan is a natural polymer derived by deacetylation of chitin, which is insoluble in usual solvents. However, when the degree of deacetylation of chitin reaches about 50%, it becomes soluble in aqueous acidic media and is called chitosan (Rinaudo, 2006). The solubility of chitosan depends on the degree of deacetylation, the distribution of acetyl groups along the main chain, the molecular weight and the nature of the acid used for protonation (Pillai, Paul, & Sharma, 2009), but it is soluble in dilute acid solutions below pH

6.0 due to the presence of amino groups. Apart from solubility, chitosan molecular weight can also affect the quality of the final film such as elasticity or brittleness (Hwang, Kim, Jung, Cho, & Park, 2003; Park, Marsh, & Rhim, 2002).

Owing to its film forming properties and antimicrobial character, chitosan is a potential material for packaging films. However, chitosan films are rigid and need plasticizers to reduce frictional forces between polymer chains, such as hydrogen bonds or ionic forces, in order to improve mechanical properties (Olabarrieta, Forsström, Gedde, & Hedenqvist, 2001; Park et al., 2002; Suyatma, Tighzert, Copinet, & Coma, 2005; Ziani, Osés, Coma, & Maté, 2008). The incorporation of polyols in the formulation of the film can overcome this drawback (Srinivasa, Ramesh, & Tharanathan, 2007) and keep film mechanical properties stable during the required time (Kerch & Korkhov, 2011; Osés, Fernández-Pan, Mendoza, & Maté, 2009).

Barrier properties in food packaging are of great importance. Interaction between oxygen or water vapour and the product could deteriorate food quality (Srinivasa, Baskaran, Ramesh, Harish Prashanth, & Tharanathan, 2002). One of the main functions of food packaging films is to retard oxygen and moisture transfer between food and the environment, so that oxygen permeability (OP) and water vapour permeability (WVP) should be as low as possible in order to increase the shelf-life of the product (Gontard, Guilbert, & Cuq, 1992).

The goal of the present work was to prepare films based on chitosans of different molecular weights to improve mechanical properties of the biofilms by the addition of glycerol. This paper mainly studied the influence of the chitosan/glycerol ratio and molecular weight of chitosan on the functional properties of the

* Corresponding author.

E-mail address: koro.delacaba@ehu.es (K. de la Caba).

films, such as mechanical and barrier properties, which are relevant for food packaging applications.

2. Materials and methods

2.1. Materials

High molecular weight (HMw) chitosan (viscosity of 800–2000 cP) and low molecular weight (LMw) chitosan (viscosity of 20–200 cP), both with a degree of deacetylation higher than 75%, were provided by Sigma–Aldrich (Spain). Acetic acid was purchased from Panreac (Spain) and was used to control solution pH. Glycerol (GLY), food grade, was used as film plasticizer and was obtained from Panreac (Spain).

2.2. Film preparation

Chitosan films were prepared by casting. A 1% by weight chitosan solution was prepared in a 1% acetic acid solution. After 15 min under continuous stirring, glycerol was added. Stirring was continued for 30 min until total homogenization of the mixture. After that, solutions were filtered and 25 mL of the solution were poured into each Petri dish and allowed to dry at room temperature. The glycerol contents employed in this study were 15 and 30 wt% of chitosan. All films were stored for 48 h in a controlled environment chamber (ACS SU700V) at 25 °C and 50% RH (relative humidity) before testing.

2.3. Film thickness

Film thickness (T) was measured to the nearest 0.001 mm with a hand-held digimatic micrometer (QuantuMike Mitutoyo). The values obtained for each sample at five different locations were averaged.

2.4. Moisture content and total soluble matter

Three specimens of each film were weighed (m_w) and subsequently dried in an air-circulating oven at 105 °C for 24 h. Films were then reweighed (m_0), to determine their moisture content (MC):

$$MC(\%) = \frac{m_w - m_0}{m_w} \times 100$$

Total soluble matter (TSM) was measured by immersion in 50 mL of distilled water. The flasks were stored in the environmental chamber at 25 °C for 24 h. After this time, specimens were dried in an air-circulating oven at 105 °C for 24 h. TSM was calculated in relation to the dry mass and it was expressed as the percentage of film dry matter solubilized. Two methods were used. In the first method the sample was dried at 105 °C for 24 h and weighed to calculate the dry matter before immersion (TSM_{dry}) (Cuq, Gontard, Cuq, & Guilbert, 1996; Kunte, Gennadios, Cuppett, Hanna, & Weller, 1997). In the second method the sample was immersed without being dried (TSM_{wet}) to avoid the effect of temperature (Rhim, Gennadios, Weller, Cezeirat, & Hanna, 1998).

2.5. Light absorption

The light-barrier properties of films were determined by measuring their light absorption at wavelengths ranging from 200 nm to 800 nm, using a UV–Jasco spectrophotometer (Model V-630). The transparency of the films was calculated by the equation A_{600}/T , where A_{600} is the absorbance at 600 nm and T is the film thickness (mm).

2.6. Colour measurements

Colour values of films were measured using a portable colorimeter (CR-400 Minolta Chroma Meter). Film specimens were placed on a white plate, and the CIELAB colour scale was used to measure colour: $L^* = 0$ (black) to $L^* = 100$ (white), $-a^*$ (greenness) to $+a^*$ (redness) and $-b^*$ (blueness) to $+b^*$ (yellowness). Standard values for the white calibration plate were $L^* = 97.39$, $a^* = 0.03$ and $b^* = 1.77$. With these values, and considering standard light source D65 and standard observer 2 degrees colour parameters, L^* , a^* , b^* were measured. The change of colour was evaluated by comparing total colour differences between films. Total colour difference (ΔE^*) was calculated as:

$$\Delta E^* = \sqrt{(L^*_{\text{standard}} - L^*_{\text{sample}})^2 + (a^*_{\text{standard}} - a^*_{\text{sample}})^2 + (b^*_{\text{standard}} - b^*_{\text{sample}})^2}$$

Values were expressed as the means of ten measurements on different areas of each film.

2.7. Fourier-transform-infrared spectroscopy (FTIR)

Fourier transformed infrared (FTIR) spectra of the films were carried out on a Nicolet Nexus FTIR spectrometer using a Golden Gate (Specac) ATR sampling accessory. A total of 32 scans were performed at 4 cm⁻¹ resolution. Measurements were recorded between 4000 and 750 cm⁻¹.

2.8. Contact angle of water

A contact angle of water (model Oca20, dataphysics instruments) was used to measure the contact angle of water in air on the surface of chitosan/glycerol films. A film sample (20 mm × 80 mm) was put on a movable sample stage and levelled horizontally; then a drop of about 3 μL of distilled water was placed on the surface of the film using a microsyringe. The contact angle was measured in a conditioned room by recording contact angle values. Image analyses were carried out using SCA20 software. Ten replicates were made per formulation.

2.9. Water vapour permeability (WVP)

WVP of the films was determined according to ASTM E96-00 (ASTM, 2000). The sample film was cut into a circle of 7.40 cm diameter and the test area was 33 cm². The setup was subjected to a temperature and relative humidity of 38 °C and 90%, respectively. Water vapour transmission rate (WVTR) was calculated as:

$$WVTR = \frac{G}{t \times A}$$

where G is the change in weight (g), t is the time (h), and A is the test area (m²). WVP was calculated as:

$$WVP = \frac{WVPR \times T}{\Delta P}$$

where T is the thickness of the test specimen (mm) and ΔP is the partial pressure difference of the water vapour across the film. WVP of three specimens for each sample was calculated and reported.

2.10. Oxygen permeability (OP)

In accordance with the method developed by Papkovsky, Papkovskaia, Smyth, Kerry, and Ogurtsov (2000), oxygen permeability was measured under controlled conditions (50 ± 3% relative humidity, 23 ± 2 °C). Films were mounted between the upper lid and rubber ring with silicone lubricant and fixed to the lower cup by screws, with an oxygen sensor housed inside. Nitrogen gas was

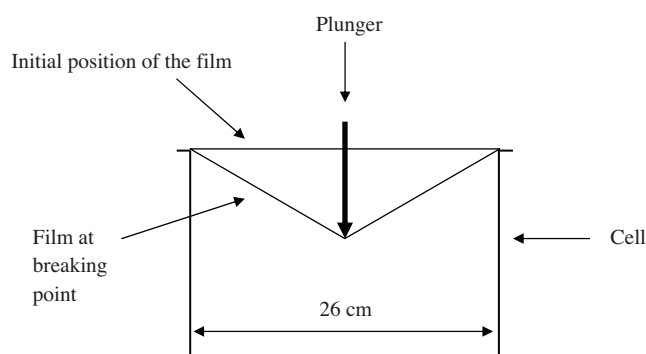


Fig. 1. Schematic diagram of puncture test carried out in this work.

blown into the chamber through one pipe, while exhausting air through another, until the nitrogen reading became stable inside the chamber. Both pipes were then shut. The sensor measured the increase in oxygen content over time. Oxygen permeability was calculated using the following equation:

$$OP = \frac{[S/(60 \cdot \beta)] \cdot (V/20.5) \cdot (273/298) \cdot [(T \cdot 1000)/A]}{101.625 \times 10^9/24}$$

where OP is the oxygen permeability ($\text{cm}^3 \mu\text{m}/\text{m}^2 \text{ day kPa}$), S is the slope, β is the permeability coefficient, A is the surface area of the film (m^2), T is the thickness of the test film samples (μm), and V is the volume of the chamber (mL).

2.11. Mechanical properties

Tensile tests were performed in an electromechanical testing system (MTS Insight 10) in order to determine tensile strength (TS) and elongation at break (EB). Tests were carried out according to ASTM D1708-93.

Puncture tests were performed to determine puncture strength (PS) and deformation (PD). In puncture testing, force is applied perpendicular to the film, as it can be seen in Fig. 1. Films were fixed in a 2.6 cm diameter cell and were perforated to breaking point using a Mecmesing Imperial 2500 testing instrument with a round-ended stainless steel plunger of 3 mm diameter and with a cross-head speed of 60 mm/min. Puncture strength and deformation were determined using Emperor software. Five replicates were tested for each composition.

2.12. Statistical analysis

The data were subjected to one-way analysis of variant (ANOVA) by means of an SPSS computer program (SPSS Statistic 17.0), while means were compared by the Tukey's test with the level of significance set at $P < 0.05$.

3. Results and discussion

At macroscopic scale, all films were homogenous and transparent, even the ones prepared without plasticizer, as shown in Fig. 2. It is worth noting that the films prepared with LMw chitosan had a slightly yellowish colour. All films had similar thickness, around 65 μm .

3.1. Moisture content and total soluble matter

Packaging films should maintain moisture levels within the packaged product. Therefore, the knowledge of moisture content and total soluble matter of the films is very important for food packaging applications. Table 1 shows the moisture content and

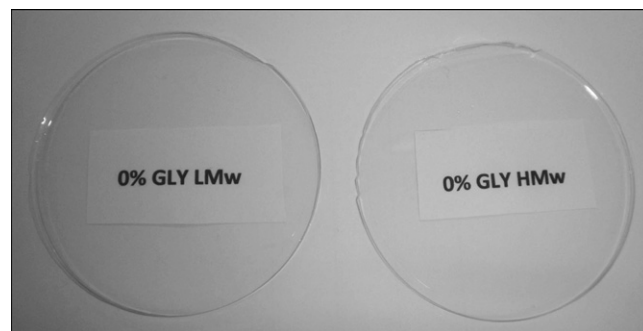


Fig. 2. Visual aspect of films without plasticizer prepared with high molecular weight (HMw) and low molecular weight (LMw) chitosans.

total soluble matter of the chitosan-based films prepared in this study.

As it is shown in Table 1, MC values are similar for films based on LMw chitosan, being around 20% ($P < 0.05$); in the case of HMw chitosan-based films, MC values increased ($P < 0.05$) when glycerol content was increased. On the other hand, TSM_{dry} values are lower ($P < 0.05$) than TSM_{wet} values, suggesting that temperature causes chemical interactions, probably produced by condensation of amino groups with the carbonyl group of the glucose reducing end groups (Fernandez-Saiz, Lagarón, & Ocio, 2009). As shown by other authors (Guerrero, Beatty, Kerry, & de la Caba, 2012), temperature promotes Maillard reaction. The early stage of the Maillard reaction involves the formation of conjugates between the carbonyl group of the reducing carbohydrate ends with the amine group in chitosan. This reaction produces a Schiff base, which subsequently cyclises to produce the Armadori compound and coloured and insoluble polymeric compounds, referred as melanoidins, are formed (Yasir, Sutton, Newberry, Andrews, & Gerardard, 2007).

Regarding to the test method, it is worth noting the high solubility of the films that were not dried before immersion, except for the films with 30% glycerol. In the case of pure chitosan films, TSM_{dry} values were 100%, indicating that they were completely soluble. Regarding to the films with 30% glycerol, TSM values were around 15% for HMw chitosan films and slightly higher, around 20% for LMw chitosan films, independent of the test method employed, indicating a good degree of interaction between the two components of the film.

Fig. 3 shows samples before and after immersion in water for 24 h. As it can be seen, chitosan/glycerol films swelled after immersion in water. Swelling was lower for the films that were heated before immersion, which indicates that temperature had influence in the structure of the films due to the fact that crosslinking between amino groups in chitosan and reducing end aldehyde carbonyl groups produces a tighter structure and leads to the yellowish colour of the sample.

Table 1

Moisture content (MC) and total soluble matter (TSM) values for chitosan-based films.

m_w	Glycerol	MC (%)	TSM_{wet} (%)	TSM_{dry} (%)
HMw	0%	15.70 ± 0.49^a	100.00 ± 0.00^a	11.39 ± 0.71^a
	15%	16.95 ± 0.24^a	100.00 ± 0.00^a	12.47 ± 1.84^a
	30%	19.24 ± 0.23^b	18.98 ± 0.32^b	15.52 ± 0.98^b
LMw	0%	19.43 ± 0.42^b	100.00 ± 0.00^a	14.40 ± 1.57^a
	15%	20.84 ± 1.14^{bc}	84.35 ± 4.70^c	20.60 ± 0.66^c
	30%	21.57 ± 0.67^c	24.30 ± 1.01^b	21.14 ± 0.62^c

Two values followed by the same letter in the same column are not significant ($P > 0.05$) different thought the Tukey's multiple range test.

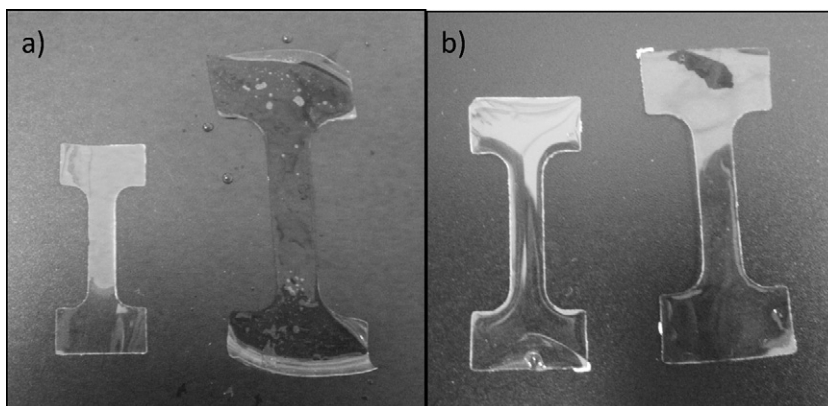


Fig. 3. Swelling capacity of LMw chitosan films prepared with 30% of glycerol: (a) when sample was directly immersed in water and (b) when sample was dried before immersion.

3.2. Light absorption

Table 2 shows the light transmission values at selected wavelengths from 200 to 800 nm and transparency for chitosan/glycerol. As it can be seen, light transmission values were almost constant regardless of the amount of glycerol. Films based on chitosan have excellent barrier properties to UV light in the UV region, regardless glycerol content. Therefore, chitosan-based films effectively prevented the UV light, so that these results suggested the potential preventive effect of chitosan films on the retardation of product oxidation induced by UV light. On the other hand, transparency is a parameter that needs to be considered for food packaging applications. All the films showed exceptional transparency that did not change with glycerol content or chitosan molecular weight.

3.3. Colour measurements

Colour values of chitosan/glycerol films at different plasticizer content are shown in Table 3. Samples were introduced in an air-circulating oven at 105 °C for 24 h and its colour change was measured in order to study the effect of temperature on the film structure. Total colour differences between films before and after being in the oven were also calculated. Films were transparent, but LMw chitosan films were slightly yellowish. It was observed that yellowness (b^*) increased ($P < 0.05$) with the addition of glycerol. When 30% of glycerol was added, it could be seen that yellowness (b^*) value increased in a remarkable way, especially for LMw chitosan films, indicating that Maillard reaction is more pronounced for these systems due to the higher reducing end content. ΔE^* results showed that colour changed in a significant way ($P < 0.05$) after being in the oven at 105 °C for 24 h for all films. As it can be observed in Fig. 4, the more glycerol content, the greater yellowness (b^*) in the case of the films dried in the oven. In contrast, there was a significant increased ($P < 0.05$) in greenness (a^*) with the addition of glycerol. Total colour difference (ΔE^*) was more

significant for LMw chitosan films and increased with the glycerol addition. Significant total colour change (ΔE^*) happened ($P < 0.05$) in all films owing to the effect of temperature. Colour parameters changed notably after introducing films in the oven at 105 °C for 24 h, which could mean that the film structure changed due to the effect of heating.

3.4. Contact angle of water

Water contact angle is a good indicator of the degree of hydrophilicity of films. The final state of a water drop on the film surface is taken as an indication of surface wettability by water. It is well known that water contact angle decreases when surface hydrophilicity is higher. To understand the effect of the plasticizer on film wettability, contact angles were investigated for chitosan films with different contents of glycerol. As it is shown in Fig. 5 water contact angles of pure chitosan films were around 105°, according to the values found in the literature (De Britto & Assis, 2007; Hsieh, Tsai, Wang, Chang, & Hsieh, 2005). There was no significant difference ($P > 0.05$) between contact angle values of pure chitosan films and films with 15% of glycerol. However, contact angle values decreased ($P < 0.05$) with the addition of 30% of glycerol due to the hydrophilic character of the plasticizer. On the other hand, the molecular weight of chitosan did not affect ($P > 0.05$) contact angle values.

It is worth noting that films with higher moisture contents had lower contact angles, indicating more ability to absorb water and so that higher hydrophilicity. Therefore, contact angle results were in good agreement with the results obtained in the moisture content test.

3.5. Fourier-transform-infrared spectroscopy (FTIR)

The FTIR spectra of pure chitosan and pure glycerol are shown in Fig. 6. The main absorption peaks of pure chitosan are observed

Table 2
Light transmission and transparency values for chitosan-based films.

m_w	Glycerol	Thickness (μm)	Light transmission (%)							Transparency A_{600}/T
			200 nm	350 nm	400 nm	500 nm	600 nm	700 nm	800 nm	
HMw	0%	0.060 ± 0.007	0.010	74.454	84.297	89.081	90.107	90.471	90.696	0.754
	15%	0.065 ± 0.004	0.011	71.908	83.133	88.561	89.680	90.112	90.381	0.732
	30%	0.063 ± 0.003	0.006	62.210	80.586	89.060	90.489	90.904	91.071	0.690
LMw	0%	0.062 ± 0.006	0.015	43.850	73.808	87.438	89.712	90.446	90.826	0.760
	15%	0.065 ± 0.004	0.014	22.590	61.641	84.544	88.216	89.281	89.742	0.838
	30%	0.068 ± 0.006	0.019	21.478	59.636	84.880	88.802	89.811	90.102	0.762

Table 3
Colour mean values (L^* , a^* and b^*) of chitosan-based films.

m_w	Glycerol	Before 24 h at 105 °C			After 24 h at 105 °C			ΔE^*
		L^*	a^*	b^*	L^*	a^*	b^*	
HMw	0%	96.39 ± 0.58 ^{ab}	−0.23 ± 0.05 ^a	3.15 ± 0.26 ^a	95.93 ± 0.39 ^a	−0.61 ± 0.02 ^a	4.72 ± 0.16 ^a	1.68 ± 0.14 ^a
	15%	97.37 ± 0.65 ^c	−0.31 ± 0.03 ^a	3.14 ± 0.06 ^a	95.66 ± 0.25 ^a	−0.91 ± 0.19 ^b	5.65 ± 0.90 ^b	3.10 ± 0.75 ^b
	30%	97.04 ± 0.84 ^c	−0.49 ± 0.05 ^b	3.86 ± 0.22 ^b	96.53 ± 0.68 ^a	−1.06 ± 0.05 ^c	6.05 ± 0.17 ^c	2.33 ± 0.24 ^c
LMw	0%	96.54 ± 0.64 ^{abc}	−0.57 ± 0.03 ^{bc}	4.74 ± 0.21 ^c	95.82 ± 0.98 ^a	−1.81 ± 0.06 ^d	9.83 ± 0.33 ^d	5.29 ± 0.39 ^d
	15%	95.72 ± 0.32 ^{ab}	−0.65 ± 0.04 ^c	4.95 ± 0.24 ^c	95.37 ± 0.34 ^a	−2.10 ± 0.03 ^e	11.59 ± 0.18 ^e	6.81 ± 0.18 ^e
	30%	94.51 ± 0.16 ^d	−1.42 ± 0.13 ^d	9.00 ± 0.73 ^d	94.13 ± 0.17 ^b	−2.94 ± 0.07 ^f	17.76 ± 0.44 ^f	8.90 ± 0.44 ^f

Two values followed by the same letter in the same column are not significant ($P > 0.05$) different through the Tukey's multiple range test.



Fig. 4. Appearance of films after being dried at 105 °C for 24 h.

at 1650 cm^{-1} , attributed to C=O stretching (amide I), at 1558 cm^{-1} , assigned to N–H bending (amide II), and at 1382 cm^{-1} , assigned C–N stretching (amide III). The absorption peak at 1050 cm^{-1} is assigned to C–O stretching and the broad band above 3000 cm^{-1} corresponds to O–H and N–H bonds (Brugnerotto et al., 2001; Fernandez-Saiz, Lagarón, & Ocio, 2007; Ziani et al., 2008).

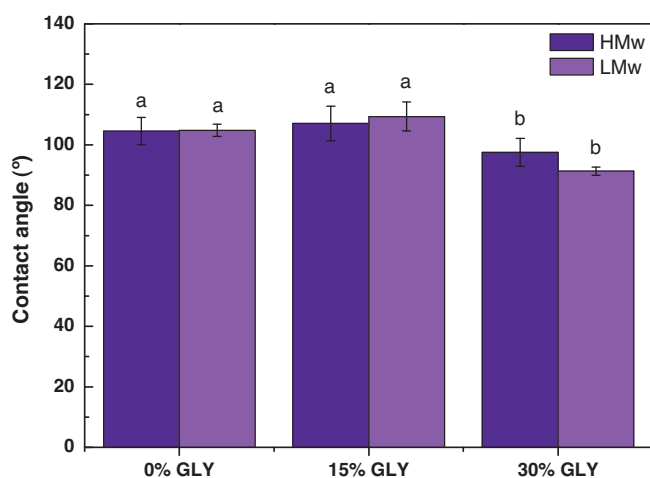


Fig. 5. Contact angle values for chitosan/glycerol films. Columns with the same letter are not significantly ($P > 0.05$) different through the Tukey's multiple range test.

The FTIR spectrum of pure glycerol shows the five typical absorption bands of glycerol located in the region from 800 cm^{-1} up to 1150 cm^{-1} , corresponding to the vibrations of C–C and C–O linkages. The peaks at 850 cm^{-1} , 925 cm^{-1} , and 995 cm^{-1} are assigned to the vibration of the skeleton C–C, the band at 1045 cm^{-1} is associated to the stretching of the C–O linkage in C1 and C3, and the one at 1117 cm^{-1} is related to the stretching of C–O in C2 (Guerrero, Retegi, Gabilondo, & de la Caba, 2010).

Fig. 7 shows FTIR spectra of chitosan/glycerol systems. The absorption peaks at 1045 cm^{-1} and 1117 cm^{-1} associated to C–O stretching joined to become a single peak when glycerol content was increased, suggesting interactions between hydroxyl groups of chitosan and glycerol by hydrogen bonding.

3.6. Barrier properties

Water vapour permeability and oxygen permeability values for chitosan/glycerol films are shown in Table 4. Chitosan films showed adequate barrier properties against water vapour for food packaging. The addition of glycerol to the system did not significantly ($P > 0.05$) influence WVP. However, WVP values were significantly ($P < 0.05$) affected by chitosan molecular weight, as it can be seen in Table 4, being slightly higher for the films prepared with LMw chitosan. These results could mean a lower degree of interaction between glycerol and chitosan than in the case of HMw chitosan, causing easier migration of water vapour molecules through the film.

Table 4

Water vapour permeability (WVP) and oxygen permeability (OP) values for chitosan-based films.

m_w	Glycerol	WVP ($\times 10^{13} \text{ g cm}^{-1} \text{ s}^{-1} \text{ Pa}^{-1}$)	OP ($\text{cm}^3 \mu\text{m m}^{-2} \text{ day}^{-1} \text{ kPa}^{-1}$)
HMw	0%	8.07 ± 1.00^a	6.65 ± 0.39^a
	15%	8.38 ± 0.21^a	20.04 ± 0.77^b
	30%	8.76 ± 0.56^a	37.38 ± 1.44^c
LMw	0%	9.21 ± 0.48^c	7.70 ± 0.72^a
	15%	10.1 ± 0.41^c	21.93 ± 0.59^b
	30%	10.2 ± 0.04^c	38.17 ± 1.49^c

Two values followed by the same letter in the same column are not significant ($P > 0.05$) different thought the Tukey's multiple range test.

On the other hand, the addition of glycerol into chitosan solutions increased ($P < 0.05$) OP values of films, as it has been also reported by other authors (Srinivasa et al., 2007). Therefore, it could be said that glycerol plasticization effect promotes the mobility of the chains, making diffusion of oxygen molecules through the film easier. Although OP values increased when glycerol content increased, the results obtained for all films were much better than OP values for commercial food packaging films used nowadays, such as low density polyethylene (LDPE) films, which have OP values around $1870 \text{ cm}^3 \mu\text{m m}^{-2} \text{ day}^{-1} \text{ kPa}^{-1}$ (Miller & Krochta, 1997). Results obtained were similar ($P > 0.05$) for films prepared with both HMw and LMw chitosans.

3.7. Mechanical properties

Mechanical properties of films are largely associated with distribution and density of intermolecular and intramolecular interactions in the network created in chitosan films. The effect of glycerol content on the mechanical properties is shown in Table 5.

Tensile strength decreased when glycerol content increased and elongation at break increased, induced by the interactions between chitosan and plasticizer, as it was shown by FTIR study.

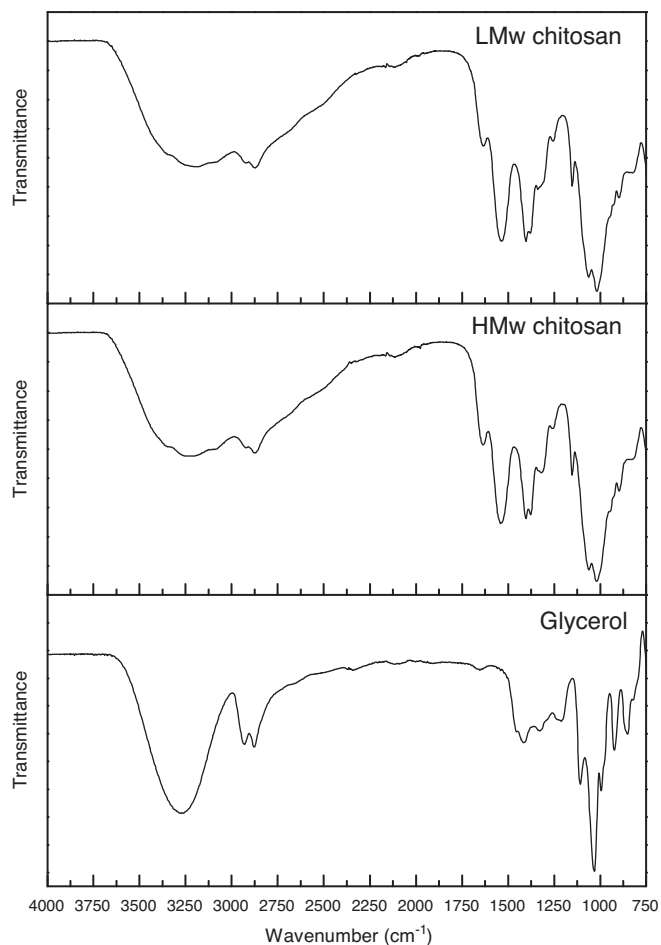


Fig. 6. Infrared spectra of pure LMw and HMw chitosans and glycerol.

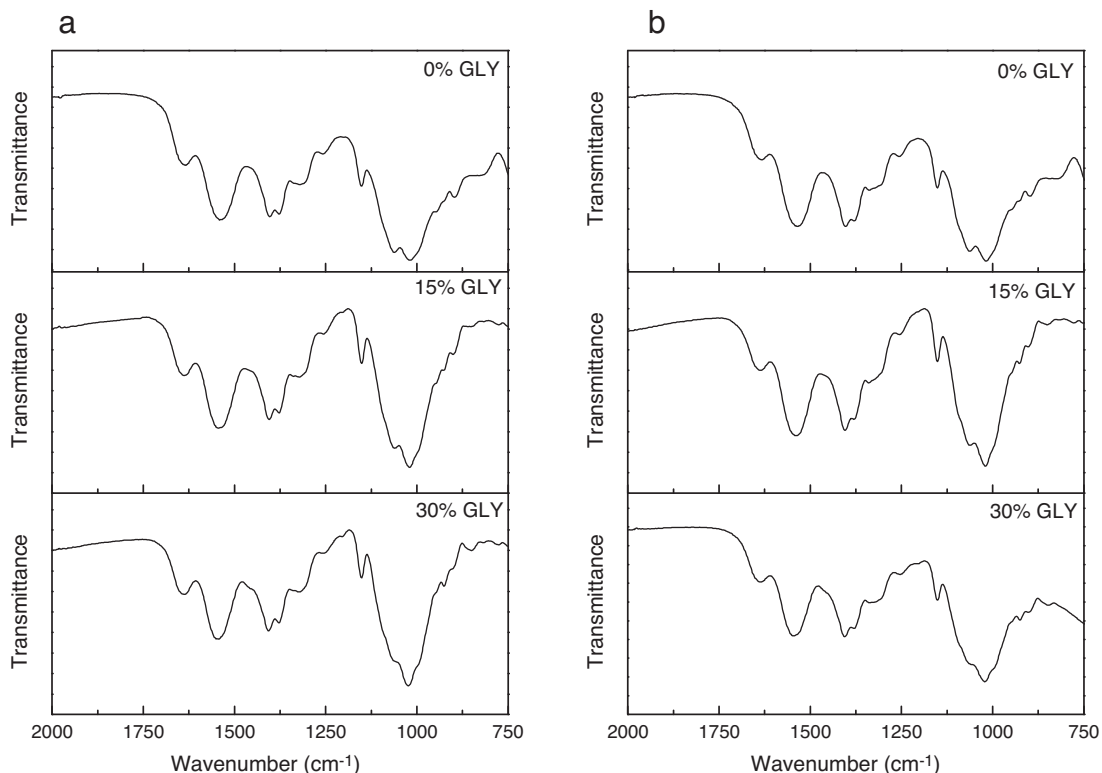


Fig. 7. Infrared spectra of chitosan/glycerol films prepared with (a) high molecular weight (HMw) and (b) low molecular weight (LMw) chitosans.

Table 5

Tensile strength (TS), elongation at break (EB), puncture strength (PS) and puncture deformation (PD) of chitosan-based films.

	Glycerol	TS (MPa)	EB (%)	PS (N)	PD (%)
HMw	0%	61.82 ± 3.43 ^a	4.59 ± 0.49 ^a	19.43 ± 0.36 ^a	8.95 ± 0.85 ^a
	15%	43.41 ± 3.11 ^b	11.14 ± 0.70 ^b	20.60 ± 0.91 ^a	12.63 ± 0.76 ^b
	30%	31.89 ± 5.93 ^c	30.51 ± 1.75 ^c	20.11 ± 2.70 ^a	17.79 ± 0.50 ^c
LMw	0%	55.83 ± 2.96 ^d	4.58 ± 0.38 ^a	12.10 ± 1.34 ^b	8.59 ± 0.87 ^a
	15%	36.85 ± 3.55 ^e	27.34 ± 3.38 ^d	11.98 ± 2.92 ^b	12.30 ± 1.40 ^b
	30%	23.87 ± 3.79 ^f	37.67 ± 2.16 ^e	12.20 ± 1.48 ^b	18.95 ± 2.12 ^c

Two values followed by the same letter in the same column are not significant ($P > 0.05$) different thought the Tukey's multiple range test.

Mechanical properties of the films can be mainly linked to the physico-chemical characteristic of the chitosan/glycerol. However, it should be also taken into account that interactions between plasticizers and chitosan could vary as a function of glycerol content. In this study tensile strength and modulus increased ($P < 0.05$) and elongation at break decreased ($P < 0.05$) when chitosan molecular weight increased. This could be due to the formation of more compact network (Chen & Hwa, 1996; Park et al., 1999).

Puncture test is a measure of the resistance of the film to be perforated. When packed product has protuberances, film should show good biaxial mechanical properties in order to maintain integrity. The ability of the plasticizer to expand chitosan chains facilitates mobility on the plane of the film. In contrast, glycerol did not have any significant effect ($P > 0.05$) in the perpendicular direction of the plane of the film. Therefore, puncture strength was maintained constant regardless the addition of glycerol. On the other hand, the plasticization effect was shown in puncture deformation results. The deformation in this test has a perpendicular component but also a component in the plane of the film (Sobral, Menegalli, Hubinger, & Roques, 2001). The addition of glycerol promotes chain mobility in the direction of the deformation, increasing puncture deformation values ($P < 0.05$) for films with higher glycerol content. Results did not show significant variations ($P > 0.05$) for the films prepared with both HMw and LMw chitosans.

4. Conclusions

The results of this work show that functional properties of chitosan-based films are adequate for packaging purposes. Films are transparent and resistant against UV light, which suggests the potential preventive effect on the retardation of product oxidation induced by UV light. In addition, films are an effective barrier against water vapour and oxygen, which helps to maintain the quality of the product. Moreover, the addition of glycerol improves film flexibility with a slight increase in the hydrophilic character of the films. These improvements in functional properties can be explained by the interactions glycerol–chitosan shown by TSM and FTIR analysis.

Acknowledgements

The authors thank MICINN (project MAT2009-07735) and UPV/EHU (project PES11/35) for their financial support, and SGiker service from the University of the Basque Country. Itsaso Leceta thanks also Basque Government (fellowship BFI-2010-82).

References

- ASTM. (1993). Standard test method for tensile properties of plastics by use of microtensile specimens, D1708-93. In *Annual book of ASTM*. Philadelphia, PA: American Society for Testing and Materials.
- ASTM. (2000). Standard test methods for water vapour transmission of material, E96-00. In *Annual book of ASTM*. Philadelphia, PA: American Society for Testing and Materials.

- Brugnerotto, J., Lizardi, J., Goycoolea, F. M., Argüelles-Monal, W., Desbrières, J., & Rinaudo, M. (2001). An infrared investigation in relation with chitin and chitosan characterization. *Polymer*, 42, 3569–3580.
- Chen, R. H., & Hwa, H. (1996). Effect of molecular weight of chitosan with the same degree of deacetylation on the thermal, mechanical, and permeability properties of prepared membrane. *Carbohydrate Polymers*, 29, 353–358.
- Cuq, B., Gontard, N., Cuq, J. L., & Guilbert, S. (1996). Functional properties of myofibrillar protein-based biopackaging as affected by film thickness. *Journal of Food Science*, 61, 580–584.
- De Britto, D., & Assis, O. B. G. (2007). A novel method for obtaining a quaternary salt of chitosan. *Carbohydrate Polymers*, 69, 305–310.
- Dutta, P. K., Tripathi, S., Mehrotra, G. K., & Dutta, J. (2009). Perspectives for chitosan based antimicrobial films in food applications. *Food Chemistry*, 114, 1173–1182.
- Fernandez-Saiz, P., Lagarón, J. M., & Ocio, M. J. (2007). Using ATR-FTIR spectroscopy to design active antimicrobial food packaging structures based on high molecular weight chitosan polysaccharide. *Journal of Agricultural and Food Chemistry*, 55, 2554–2562.
- Fernandez-Saiz, P., Lagarón, J. M., & Ocio, M. J. (2009). Optimization of the film-forming and storage conditions of chitosan as an antimicrobial agent. *Journal of Agricultural and Food Chemistry*, 57, 3298–3307.
- Gontard, N., Guilbert, S., & Cuq, J. L. (1992). Edible wheat gluten films: Influence of the main process variables on film properties using response surface methodology. *Journal of Food Science*, 57, 190–195.
- Guerrero, P., Beatty, E., Kerry, J. P., & de la Caba, N. K. (2012). Extrusion of soy protein with gelatin and sugars at low moisture content. *Journal of Food Engineering*, 110, 53–59.
- Guerrero, P., Retegi, A., Gabilondo, N., & de la Caba, K. (2010). Mechanical and thermal properties of soy protein films processed by casting and compression. *Journal of Food Engineering*, 100, 145–151.
- Hsieh, C. H., Tsai, S.-P., Wang, D. M., Chang, Y. N., & Hsieh, H. J. (2005). Preparation of c-PGA/chitosan composite tissue engineering matrices. *Biomaterials*, 26, 5617–5623.
- Hwang, K. T., Kim, J. T., Jung, S. T., Cho, G. S., & Park, H. J. (2003). Properties of chitosan-based biopolymer films with various degrees of deacetylation and molecular weights. *Journal of Applied Polymer Science*, 89, 3476–3484.
- Kerch, G., & Korkhov, V. (2011). Effect of storage time and temperature on structure, mechanical and barrier properties of chitosan-based films. *European Food Research and Technology*, 232, 17–22.
- Kunte, L. A., Gennadios, A., Cuppett, S. L., Hanna, M. A., & Weller, C. L. (1997). Cast films from soy protein isolates and fractions. *Cereal Chemistry*, 74, 115–118.
- Miller, K. S., & Krochta, J. M. (1997). Oxygen and aroma barrier properties of edible films: A review. *Trends in Food Science and Technology*, 8, 228–237.
- Olabarrieta, I., Forsström, D., Gedde, U. W., & Hedenqvist, M. S. (2001). Transport properties of chitosan and whey blended with poly(ϵ -caprolactone) assessed by standard permeability measurements and microcalorimetry. *Polymer*, 42, 4401–4408.
- Osés, J., Fernández-Pan, I., Mendoza, M., & Maté, J. I. (2009). Stability of the mechanical properties of edible films based on whey protein isolate during storage at different relative humidity. *Food Hydrocolloids*, 23, 125–131.
- Papkovsky, D. P., Papkovskaia, N., Smyth, A., Kerry, J., & Ogurtsov, V. O. (2000). Phosphorescent sensor approach for non-destructive measurement of oxygen in packaged foods: Optimisation of disposable oxygen sensors and their characterization over a wide temperature range. *Analytical Letters*, 33, 1755–1777.
- Park, H. J., Jung, S. T., Song, J. J., Kang, S. G., Vergano, P. J., & Testin, R. F. (1999). Mechanical and barrier properties of chitosan-based biopolymer film. *Chitin and Chitosan Research*, 5, 19–26.
- Park, S. Y., Marsh, K. S., & Rhim, J. W. (2002). Characteristics of different molecular weight chitosan film affected by the type of organic solvents. *Journal of Food Science*, 67, 194–197.
- Pillai, C. K. S., Paul, W., & Sharma, C. P. (2009). Chitin and chitosan polymers: Chemistry, solubility and fiber formation. *Progress in Polymer Science*, 34, 641–678.
- Rhim, J. W., Gennadios, A., Weller, C. L., Cezeirat, C., & Hanna, M. A. (1998). Soy protein isolate-dialdehyde starch films. *Industrial Crops and Products*, 8, 195–203.
- Rinaudo, M. (2006). Chitin and chitosan: Properties and applications. *Progress in Polymer Science*, 31, 603–632.

- Sobral, P. J., Menegalli, F. C., Hubinger, M. D., & Roques, M. A. (2001). Mechanical, water vapour barrier and thermal properties of gelatine based edible films. *Food Hydrocolloids*, 15, 423–432.
- Srinivasa, P. C., Baskaran, R., Ramesh, M. N., Harish Prashanth, K. V., & Tharanathan, R. N. (2002). Storage studies of mango packed using biodegradable chitosan film. *European Food Research and Technology*, 215, 504–508.
- Srinivasa, P. C., Ramesh, M. N., & Tharanathan, R. N. (2007). Effect of plasticizers and fatty acids on mechanical and permeability characteristics of chitosan films. *Food Hydrocolloids*, 21, 1113–1122.
- Suyatma, N. E., Tighzert, L., Copinet, A., & Coma, V. (2005). Effect of hydrophilic plasticizers on mechanical, thermal, and surface properties of chitosan films. *Journal of Agricultural and Food Chemistry*, 53, 3950–3957.
- Yasir, B. M., Sutton, K. H., Newberry, M. P., Andrews, N. R., & Gerardard, J. A. (2007). The impact of Maillard crosslinking on soy proteins ad tofu texture. *Food Chemistry*, 104, 1502–1508.
- Ziani, K., Oses, J., Coma, V., & Maté, J. I. (2008). Effect of the presence of glycerol and Tween 20 on the chemical and physical properties of films based on chitosan with different degree of deacetylation. *LWT – Food Science and Technology*, 41, 2159–2165.